Applied Physics Letters ARTICLE scitation.org/journal/apl

# Picosecond ultrasounds as elasticity probes in neuron-like cells models

Cite as: Appl. Phys. Lett. **115**, 213701 (2019); doi: 10.1063/1.5129783
Submitted: 1 October 2019 · Accepted: 7 November 2019 ·
Published Online: 18 November 2019



Alexis Viel,[1,2] Emmanuel Péronne,[1] Océane Sénépart,[2,3,4] Loïc Becerra,[1] Claire Legay,[3] Fannie Semprez,[3] Léa Trichet,[2] Thibaud Coradin,[2] Ahmed Hamraoui,[2,5,a)] and Laurent Belliard[1]

## AFFILIATIONS

[1]Sorbonne Université, CNRS UMR7588, Institut des Nanosciences de Paris, 4 place Jussieu, 75005 Paris, France
[2]Sorbonne Université, CNRS UMR7574, Laboratoire de Chimie de la Matiére Condensée de Paris, 4 place Jussieu, 75005 Paris, France
[3]Saints-Péres Paris Institute for the Neurosciences, CNRS UMR8003, Université de Paris, Paris Descartes, Faculté des Sciences Fondamentales et Biomédicales, 45 rue des Saints-Péres, 75006 Paris, France
[4]Centre de recherche de l'ECE Paris-Lyon, Immeuble Pollux-37 quai de Grenelle-CS 71520-75015 Paris, France
[5]Université de Paris, Paris Descartes, Faculté des Sciences Fondamentales et Biomédicales, 45 rue des Saints-Péres, 75006 Paris, France

[a)]**Electronic mail:** ahmed.hamraoui@sorbonne-universite.fr

## ABSTRACT

We report on elasticity measurements in neuronlike cells using picosecond acoustics pump and probe spectroscopy. The stimulated Brillouin oscillations were mapped in PC12 cells to reveal their internal elastic structure. Thanks to a Pearson correlation coefficient mapping, different areas could be distinguished. The nucleus material shows a bulk modulus equal to 12.9 GPa in the case of a dry cell. Attenuation of the Brillouin signature gives access to dynamical longitudinal viscosity equal to 10.6 mPa · s, one order of magnitude higher than that of water. The modulus considerably drops to 2.6 GPa in the most physiologically relevant case of a hydrated cell.



Cells respond to mechanical signals perceived from the nearest extracellular world.[1–4] For instance, it has been suggested that mechanical constraints prevail over biochemical signaling in the early stage of embryogenesis.[5] Substrate stiffness has also been identified as a key factor driving cell proliferation and differentiation.[6] Both endothelial and smooth muscle cells were shown to proliferate in response to stretching; however, in the case of endothelial cells, this response depends on cell-cell adhesion.[7] In the mechanotransduction process, external forces exerted on the cells transit inside them through microscale adhesion domains that serve as anchoring points for the structuration of the cellular cytoskeletal network. This phenomenon allows the cell to sense its surrounding environment and is followed by the activation of fundamental cellular processes involving motility or changes in the cell shape.[8] Obviously, how this regulation occurs will depend on the cell type and function. In the case of tumors, the increase in rigidity could be related to various factors, including an increase in the modulus of elasticity of transformed cells due to cellular disturbances. This leads to tumors being generally stiffer than normal tissues.[9,10]

Perturbation of tissue rigidity is associated with different types of pathology. However, it is sometimes difficult to conclude if this change in stiffness of cells or tissue is the effect or the source of the pathologies.[11] This is why the characterization of the mechanical properties of cells is essential to understand their behavior during mitosis, apoptosis, adhesion, mobility, and disease development.[12–14] However, the complexity of the inner cell composition and the intricate meshwork formed by molecular mediators of the transmembrane cell-substrate interactions requires noninvasive techniques to probe and quantify local mechanical properties of cells, including modulus of elasticity, viscoelastic properties, adhesion, and forces created at the single-cell scale. Several recent reviews describe tools used to study cell mechanics[15,16] and to apply forces on them.[17] The vast majority of conventional methods of measuring the local mechanical properties of cells are based on the use of solid probes, such as AFM, and as a result, the measured mechanical properties can strongly depend on the contact/adhesion between the probe and the cell.

In contrast, acoustic waves generated by lasers provide a very adequate tool for probing the mechanical properties of biological cells or tissues in a noncontact, noninvasive configuration. In the optical pump probe technique usually called picosecond acoustics (PA), high frequency acoustic pulses (in the 1–1000 GHz range) can be generated by the pump beam and detected using a delayed probe beam. Since acoustic waves travel several microns per nanosecond, it is possible to study material on a submicron scale with acoustic waves of 10 GHz or more. Such time resolved measurements are known to achieve sound velocity characterization with an accuracy less than <5 %, parameter directly related to the elasticity behavior. In addition, by combining the time and space aspects, it is possible to perform 3D elastic investigations with a submicrometer resolution. To finish, the all-optical approach allows us to consider complex environments to address issues related to relevant biological conditions, aqueous media, and controlled temperature. For more than 30 years, properties of matter, mainly solid thin metallic films and transparent media, have been probed at the microscale using PA.[18] Ten years ago, this technique was adapted to the study of whole cells.[19,20] Since then, PA experiments have been performed in various configurations to characterize the cell/substrate interactions at the cell scale. For example, the physical properties of the contact between the cell and the substrate have been investigated[21,22] by characterizing the reflected acoustic pulses. In-depth studies of the elastic properties have also been reported in cells for single point measurements.[23,24] Full mapping of a whole cell using Brillouin frequency (BF) has been achieved *in vitro*[25] and more significantly on living cells.[26–28] Indeed, during PA experiments, the cell reflectivity is time-dependent and exhibits a decaying oscillating behavior, called the Brillouin oscillations (BOs). Since the BO frequency is related to the sound velocity and the decaying time is related to the viscosity, the time domain investigation of BO signature can be used to carry out an in-depth study of the elastic properties.[29] Recently, a multi parametric elastic mapping in mitotic macrophage cells has been reported,[30] illustrating how the various PA configurations can bring correlative information's to cell investigations.

In this paper, detection of BO allowed for mapping elastic properties in single neuronlike cells. To our knowledge, this is the first time this technique is used on these types of cells, in which the regeneration processes are closely related to cell elasticity.

The elasticity contrasts thus revealed between the nucleus and the cytoskeleton in the reticulate cells also obviously exist in living cells for which the study is more subtle given the very specific conditions necessary for their maintenance. PC12 cells constitute a standard model for adhesion and neuronal differentiation studies.[31–35] The frequencies and the lifetimes of the BOs are mapped across the cell using the Pearson correlation method. Finally, the influence of hydration, *i.e.*, in more biologically relevant conditions, on the cell elasticity is investigated.

PC12 cells were routinely maintained following the procedure described in previously by Lamour *et al.*[32–35] PC12 cells cultured on "Ti-$SiO_2$" substrates were fixed using glutaraldehyde/paraformaldehyde (2% in phosphate buffered saline (PBS)) at room temperature during 20 min. Then, cells were washed twice with PBS for 5 min and rinsed with de-ionized water to remove salts.

In order to avoid possible cell overheating induced by the energetic pump beam, PC12 cells were grown on specific substrates. A 10 $\mu$m thick membrane was obtained by anisotropic etching of silicon, and a 100 nm *Ti* layer was sputtered on the both sides of the silicon substrate to create an acoustic transducer excited by the pump beam at the bottom side and a cytocompatible top surface for cell adhesion [Fig. 1(a)]. In this way, working at a modulation frequency of 1.8 MHz, the thermal diffusion length in the silicon substrate is much smaller than its thickness, which reduces the rise of the temperature in the PC12 cells deposited on the other top side, which is induced by the pump beam on the bottom side. The experimental setup used in this study operating in reflection geometry in an inverted Olympus microscope has been detailed in previous work.[36,37] A lock-in detection scheme is used to measure the change of sample reflectivity induced by the pump beam. Both pump and probe beams are focused around 2 $\mu$m diameter at $1/e^2$. Typical beam powers used in this experiment are 300 $\mu$W for the pump beam and 50 $\mu$W for the probe beam.

After an accurate pump and probe alignment, the sample is translated by a piezoelectric stage in order to locate the PC12 cell. Figure 1(b) shows an optical image of the cell reflectivity provided by the DC component of the signal after reflection. The acoustic signals (b)–(d) are provided by the AC component of the signal as extracted by the lock-in amplifier. The red dots point to the different locations where the acoustic signal has been recorded. The comparison between Figs. 1(c) and 1(d) shows that a decaying oscillation appears when the probe beam is located in the central region of the cell. Named Brillouin oscillations (BOs), they arise from the interference between the probe beam reflected at the sample surface and the probe beam reflected by the transient acoustic pulse that propagates into the cell. It is remarkable that the frequency and the lifetime of the oscillation vary with the location of the measurement point, as illustrated in Figs. 1(d) and 1(e). Assuming that the refractive index of the cell is real and constant $n_{cell} = 1.37 - 1.39$[38] through the cell, a fluctuation of elasticity inside the cell can be mapped. Given that the BO frequency is equal to $f_b = \frac{2nv}{\lambda}$, the change of frequency can be correlated with the fluctuation of the sound velocity $v$. Moreover, assuming a constant mass density $\rho = 1\,\mathrm{g.cm^{-3}}$ across the cell, the fluctuation of the dynamical

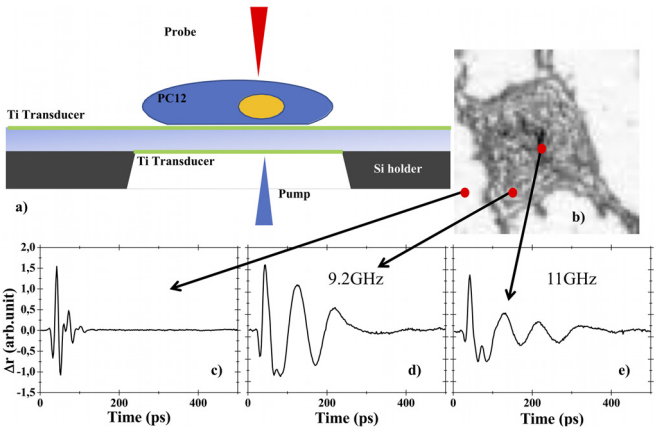


**FIG. 1.** (a) Schematic of sample geometry. The thickness of the top silicon device is 10 $\mu$m. The wavelengths of the pump and the probe are 400 and 800 nm, respectively. (b) Raw optical reflectivity image of a PC12 cell. The red squares indicate the position of the 3 points where differential optical reflectivity is measured (c) outside the cell and (d) and (e) inside the cell. (b) No BO measured on the Ti parts. (d) and (e) The BO arises within the cell only and shows fluctuation from point to point inside the cell.

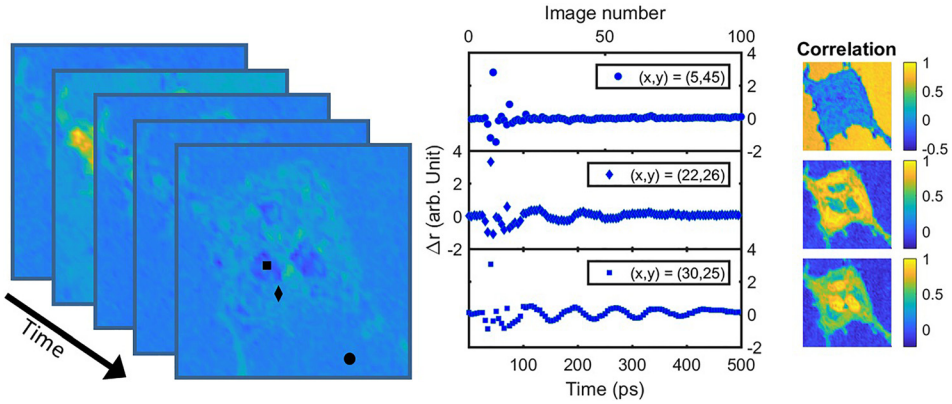


**FIG. 2.** Left: typical images obtained on a PC12 cell at different pump-probe time delays (5 ps time step). Lateral scale: 60 $\mu$m. Middle: examples of time dependence of the reflectivity for 3 different pixel's coordinates $(x,y)$ extracted from the image sequence (see the corresponding symbols). Right: Pearson correlation coefficient maps associated with the three chosen pixels.

longitudinal viscosity $\mu$ can be evaluated as well, given that the lifetime of the BO is expressed as $\tau = \frac{\rho v^2}{4\pi^2 f_B^2 \mu}$.[39]

In order to map the variation of the mechanical properties within the cell, the change of reflectivity has been measured for different pump-probe delays and locations, as sketched in Fig. 2. By comparing the time dependent signals measured at different pixels like the ones displayed in Fig. 2, the signals can be evaluated as the sum of two distinct ones. The first signal is the BOs that arise whenever the cell is probed. The second one is the transient feature that occurs repeatedly with decaying amplitude every 31 ps. It corresponds to the longitudinal waves emerging at the top free surface, which have been generated by the pump at the bottom interface and have propagated back and forth through the titanium layer before propagating through the cell. When the probe beam is not located in the cell, these transient features are the only contribution to the reflectivity signal as illustrated in Fig. 1(c). The acoustic echo signal appears to be constant everywhere, while the BO part can change drastically from pixel to pixel. Given the temporal signature of the signal between different pixels, it is possible to calculate the cross correlation between pixels to evaluate the similarity between them and then to sort out the pixels. The Pearson correlation coefficient (Pcc) between one pixel and all the others has been computed for three different pixels (see maps on the right-hand side of Fig. 2). It allows the clear identification of the regions without (top map) or with cells. Moreover, the Pcc maps of the pixels chosen within the cell shed light on inner cellular structures associated with different BOs when comparing the middle and bottom Pcc maps.

In order to confirm the existence of inner cell acoustic features, we have performed a least squares fit of the BO signal with an exponentially decaying cosine function for all the time traces recorded within the cell. The acoustic echo contribution, averaged over the titanium region, has been subtracted prior to the fitting procedure. Figure 3(a) displays a typical BO signal recorded within the cell with its corresponding fit curve. The fit parameters are the exponential decay time $\tau$, the cosine amplitude, the cosine frequency $f_B$, and the cosine phase. The occurrence of the fitted BF $f_B$ is plotted in Fig. 3(b). The distribution displays a bimodal shape, which can be fitted with a sum of two Gaussian functions. The fit suggests the presence of different inner structures associated with different Brillouin frequencies.

A close inspection of the BF distribution [see Fig. 3(b)] reveals that a fair number of pixels associated with low frequency ($f_B < 9.0$ GHz) is not well accounted for the Gaussian fit of the frequency distribution. Let us divide the frequency domain into three bands: one band centered at $f_B = 12.4$ GHz and 1.0 GHz wide, another domain centered at $f_B = 10.45$ GHz and 2.9 GHz wide; and the last domain such that $f_B < 9.0$ GHz. The cell acoustic properties can now be mapped according to the BF as shown in Fig. 4. The inner structures revealed by the Pcc maps are confirmed by the Brillouin frequencies mapping. The high BF domain centered at 12.4 GHz correlates with the nucleuslike features, while the middle frequency domain centered at 10.45 GHz would correspond to the cytoplasm. It is important to emphasize that these structures are not distinguishable in the raw reflectivity image presented in Fig. 1(b). The nuclei exhibit a higher bulk modulus $B = \rho v^2$ than the rest of the cell: 12.9 GPa compared to 9.1 GPa, respectively. The presence of three nuclei suggests that the studied object is not a single cell but rather the agglomeration of three PC12 cells.

The typical signal of each frequency domain (i.e., region of the map) is obtained by averaging the signal over the blue, red, and green dot distribution shown in the map. The results are plotted in Fig. 5(a). As expected, the pixels located at the periphery are associated on average to a decaying time shorter than the Brillouin oscillation period. Indeed, the Brillouin detection mechanism is not expected to be very

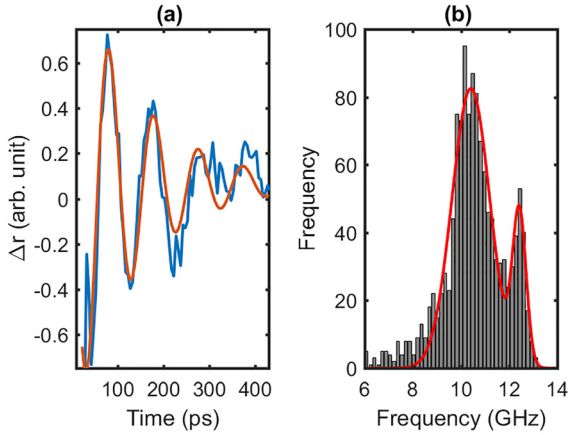


**FIG. 3.** (a) Typical Brillouin oscillation signal obtained inside the cell. The signal is fitted with exponentially decaying cosin function (red line). (b) Frequency distribution of the fitted Brillouin frequencies. The distribution is fitted with a sum of two Gaussian functions (red line).

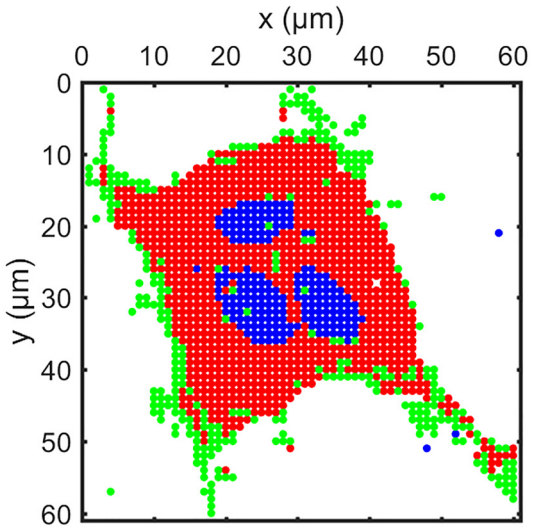


**FIG. 4.** Cell mapping according to the fitted frequency $f_B$(GHz). Blue dots: $11.9 < f_B < 12.9$. Red dots: $9.0 < f_B < 11.9$. Green dots: $f_B < 9.0$.

efficient on the edges of the cell or on the neurite because the cell thickness becomes comparable to or smaller than the acoustic wavelength (≈400 nm). In this case, the short lifetimes are not directly related to viscosity but are mainly determined by the thickness of the probed biological material. Further development will be needed to obtain elastic information on specific areas using approaches described by Liu *et al.*[30] The BO associated with the nucleus is lasting longer than the BO associated with the cytoplasm. This trend is detailed in Fig. 5(b), which plots the cumulated frequency distribution of the fitted lifetime. Nucleus lifetimes are scattered on the long lifetime part of the distribution (blue bars), while the edge lifetimes are scattered on the lower part of the distribution (green bars). The surrounding cytoskeleton lifetimes are lying in between. The dynamical longitudinal viscosity can be estimated: the extracted value for the nucleus is equal to 10.6 mPa s, much larger than in water (1 mPa s), which is in good agreement with the viscosity value deduced from the motion of organelles transported by motor proteins within cells using fluorescence microscopy.[40] The surrounding cytoskeleton has a higher viscosity estimated at 14.1 mPa s. The uncertainty on the viscosity values is estimated at 30% related to the fluctuation of BO lifetime on the areas of interest.

Although live cells[25,27] have been recently probed, such experiments imply complex setups so that most of the studies using PA to probe biological objects have involved fixed dried cells. As an intermediate situation, we probed the cell in a hydrated state.

In Fig. 6, three signals are shown, BO in the hydrating liquid and BO in the cell either hydrated or dried. For all samples, the reflectivity signal has the overall same shape as the one observed previously: an acoustical pulse followed by an oscillation. The frequency of the BO of water is 5.3 GHz (i.e., longitudinal sound velocity around 1550 $m \cdot s^{-1}$), whereas this value is almost twice higher, 10 GHz, in the dry cell. When the cell is hydrated, this value drops to 5.6 GHz (i.e., longitudinal sound velocity around 1630 $m \cdot s^{-1}$), close to the one of water. Assuming that the refractive index of the probed cell does not change with the hydration, such a drop of the value of BF shows the key role played by the hydrating liquid in the mechanical properties of the cell. The value of the average bulk moduli is found around 2.6 GPa close to that of water[25] and smaller than in the dry cell. In addition, from the lifetime of the BO oscillations estimated at 500 ps, i.e., 2–3 times greater than for the fixed cells, we can estimate a much lower viscosity for the hydrated cells around 4.2 mPa·s.

In conclusion, a special transducer was designed in order to launch and detect gigahertz acoustic waves within the cell using the pump probe technique. We demonstrated that the pump and probe spectroscopy approach coupled with Pearson correlation is a powerful tool to investigate the inner elastic features in PC12 neuronlike cells such as bulk modulus and dynamical longitudinal viscosity. Mapping the Brillouin oscillation allowed us to distinguish areas with different

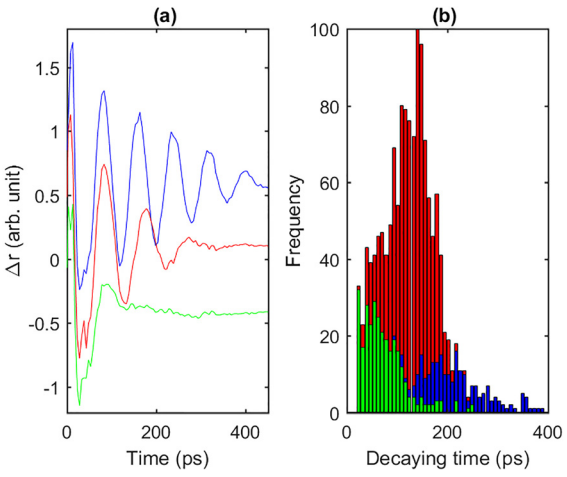


**FIG. 5.** (a) Brillouin oscillation signal averaged over three different spectral ranges. Blue curve: $11.9\ GHz < f_B < 12.9\ GHz$. Red curve: $9.0\ GHz < f_B < 11.9\ GHz$. Green curve: $f_B < 9.4\ GHz$ and $f_B > 12.9\ GHz$. (b) Cumulative bar plot of the occurrence of the decaying times corresponding to the three spectral ranges.

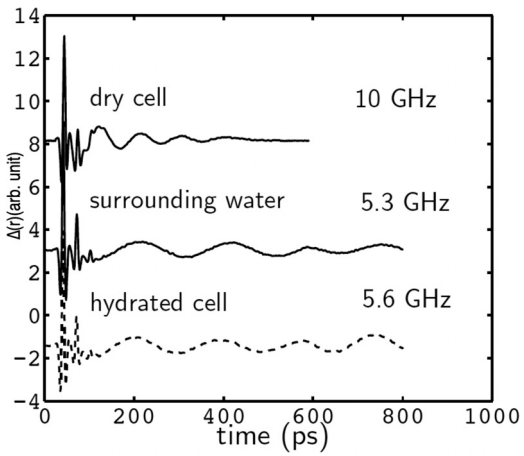


**FIG. 6.** Comparison between time resolved signatures in the dry cell (top), aqueous medium (middle), and hydrated cell (bottom). The BO frequency in hydrated cell drops significantly toward the value of the solution.

local elastic properties inside the probed biological object. Those areas have been identified as specific parts of the cell, for instance, areas exhibiting high stiffness and viscosity were assimilated to the nucleus. In the PC12 case, we report a large bulk modulus contrast (∼30 %) between the nucleus and the surrounding cytoskeleton. We also highlight the effect of hydration on the elasticity of cells, which opens the door to the study of these systems in living conditions. Combining this approach with other reported methods on different biological objects might bring new interesting results in the future.

The authors wish to thank Sorbonne University's Emergence program for its financial support involving LCMCP and INSP.

## REFERENCES


[1]N. Wang, J. D. Tytell, and D. E. Ingber, "Mechanotransduction at a distance: Mechanically coupling the extracellular matrix with the nucleus," Nat. Rev. Mol. Cell Biol. **10**, 75–82 (2009).

[2]A. Buxboim, I. L. Ivanovska, and D. E. Discher, "Matrix elasticity, cytoskeletal forces and physics of the nucleus: How deeply do cells 'feel'outside and in?," J. Cell Sci. **123**(3), 297–308 (2010).

[3]A. J. Engler, S. Sen, H. L. Sweeney, and D. E. Discher, "Matrix elasticity directs stem cell lineage specification," Cell **126**(4), 677–689 (2006).

[4]N. Huebsch, P. R. Arany, A. S. Mao, D. Shvartsman, O. A. Ali, S. A. Bencherif, J. Rivera-Feliciano, and D. J. Mooney, "Harnessing traction-mediated manipulation of the cell/matrix interface to control stem-cell fate," Nat. Mater. **9**, 518–526 (2010).

[5]D. E. Discher, P. Janmey, and Y. L. Wang, "Tissue cells feel and respond to the stiffness of their substrate," Science **310**, 1139–1143 (2005).

[6]R. Fickentscher, P. Struntz, and M. Weiss, "Mechanical cues in the early embryogenesis of caenorhabditis elegans," Biophys. J. **105**, 1805–1811 (2013).

[7]W. F. Liu, C. M. Nelson, J. L. Tan, and C. S. Chen, "Cadherins, RhoA, and Rac1 are differentially required for stretch-mediated proliferation in endothelial versus smooth muscle cells," Circ Res **101**, e44 (2007).

[8]F. Chowdhury, S. Na, D. Li, Y.-C. Poh, T. S. Tanaka, F. Wang, and N. Wang, "Material properties of the cell dictate stress-induced spreading and differentiation in embryonic stem cells," Nat. Mater. **9**, 82–88 (2010).

[9]M. Beil, A. Micoulet, G. von Wichert, S. Paschke, P. Walther, M. Bishr Omary, P. P. Van Veldhoven, U. Gern, E. Wolff-Hieber, J. Eggermann, J. Waltenberger, G. Adler, J. Spatz, and T. Seufferlein, "Sphingosylphosphorylcholine regulates keratin network architecture and visco-elastic properties of human cancer cells," Nat. Cell Biol. **5**, 803–811 (2003).

[10]J. Margueritat, A. Virgone-Carlotta, S. Monnier, H. Delanoë-Ayari, H. C. Mertani, A. Berthelot, Q. Martinet, X. Dagany, C. Rivière, J.-P. Rieu, and T. Dehoux, "High-frequency mechanical properties of tumors measured by Brillouin light scattering," Phys. Rev. Lett. **122**, 018101 (2019).

[11]G. Bao and S. Suresh, "Cell and molecular mechanics of biological materials," Nat. Mater. **2**, 715–725 (2003).

[12]C. Zhu, G. Bao, and N. Wang, "Cell mechanics: Mechanical response, cell adhesion, and molecular deformation," Annu. Rev. Biomed. Eng. **2**, 189–226 (2000).

[13]S. Suresh, J. Spatz, J. P. Mills, A. Micoulet, M. Dao, C. T. Lim, M. Beil, and T. Seufferlein, "Connections between single-cell biomechanics and human disease states: Gastrointestinal cancer and malaria," Acta Biomater. **1**, 15–30 (2005).

[14]S. Suresh, "Biomechanics and biophysics of cancer cells," Acta Biomater. **3**, 413–438 (2007).

[15]D.-H. Kim, P. K. Wong, J. Park, A. Levchenko, and Yu. Sun, "Microengineered platforms for cell mechanobiology," Annu. Rev. Biomed. Eng. **11**, 203–233 (2009).

[16]R. M. Hochmuth, "Micropipette aspiration of living cells," J. Biomech. **33**, 15–22 (2000).

[17]T. D. Brown, "Techniques for mechanical stimulation of cells in vitro: A review," J. Biomech. **33**, 3–14 (2000).

[18]C. Thomsen, H. T. Grahn, H. J. Maris, and J. Tauc, "Surface generation and detection of phonons by picosecond light pulses," Phys. Rev. B **34**, 4129–4138 (1986).

[19]T. Dehoux, M. Abi Ghanem, O. F. Zouani, M. Ducousso, N. Chigarev, C. Rossignol, N. Tsapis, M.-C. Durrieu, and B. Audoin, "Probing single-cell mechanics with picosecond ultrasonics," Ultrasonics **56**, 160–171 (2015).

[20]C. Rossignol, N. Chigarev, M. Ducousso, B. Audoin, G. Forget, F. Guillemot, and M. C. Durrieu, "In vitro picosecond ultrasonics in a single cell," Appl. Phys. Lett. **93**, 123901 (2008).

[21]T. Dehoux, M. Abi Ghanem, O. F. Zouani, J.-M. Rampnoux, Y. Guillet, S. Dilhaire, M.-C. Durrieu, and B. Audoin, "All-optical broadband ultrasonography of single cells," Sci. Rep. **5**, 8650 (2015).

[22]M. Abi Ghanem, T. Dehoux, L. Liu, G. Le Saux, L. Plawinski, M.-C. Durrieu, and B. Audoin, "Opto-acoustic microscopy reveals adhesion mechanics of single cells," Rev. Sci. Instrum. **89**, 014901 (2018).

[23]A. Gadalla, T. Dehoux, and B. Audoin, "Transverse mechanical properties of cell walls of single living plant cells probed by laser-generated acoustic waves," Planta **239**, 1129–1137 (2014).

[24]O. F. Zouani, T. Dehoux, M.-C. Durrieu, and B. Audoin, "Universality of the network-dynamics of the cell nucleus at high frequencies," Soft Matter **10**, 8737–8743 (2014).

[25]S. Danworaphong, M. Tomoda, Y. Matsumoto, O. Matsuda, T. Ohashi, H. Watanabe, M. Nagayama, K. Gohara, P. H. Otsuka, and O. B. Wright, "Three-dimensional imaging of biological cells with picosecond ultrasonics," Appl. Phys. Lett. **106**, 163701 (2015).

[26]F. Pérez-Cota, R. J. Smith, E. Moradi, L. Marques, K. F. Webb, and M. Clark, "Thin-film optoacoustic transducers for subcellular Brillouin oscillation imaging of individual biological cells," Appl. Opt. **54**, 8388 (2015).

[27]F. Pérez-Cota, R. J. Smith, E. Moradi, L. Marques, K. F. Webb, and M. Clark, "High resolution 3D imaging of living cells with sub-optical wavelength phonons," Sci. Rep. **6**, 39326 (2016).

[28]F. Perez-Cota, R. J. Smith, H. M. Elsheikha, and M. Clark, "New insights into the mechanical properties of acanthamoeba castellanii cysts as revealed by phonon microscopy," Biomed. Opt. Express **10**, 2399–2408 (2019).

[29]V. E. Gusev and P. Ruello, "Advances in applications of time-domain Brillouin scattering for nanoscale imaging," Appl. Phys. Rev. **5**, 031101 (2018).

[30]L. Liu, L. Plawinski, M.-C. Durrieu, and B. Audoin, "Label-free multiparametric imaging of single cells: Dual picosecond optoacoustic microscopy," J. Biophotonics **12**(8), e201900045 (2019).

[31]L. A. Greene and A. S. Tischler, "Establishment of a noradrenergic clonal line of rat adrenal pheochromocytoma cells which respond to nerve growth factor," Proc. Natl. Acad. Sci. U.S.A. **73**, 2424–2428 (1976).

[32]G. Lamour, S. Souès, and A. Hamraoui, "Interplay between long- and short-range interactions drives neuritogenesis on stiff surfaces," J. Biomed. Mater. Res., Part A **99**(4), 598–606 (2011).

[33]G. Lamour, S. Souès, and A. Hamraoui, "Substrate-induced PC12 cell differentiation without filopodial, lamellipodial activity or ngf stimulationa," Macromol. Biosci. **15**(3), 364–371 (2015).

[34]G. Lamour, N. Journiac, S. Souès, S. Bonneau, P. Nassoy, and A. Hamraoui, "Influence of surface energy distribution on neuritogenesis," Colloids Surf., B **72**(2), 208– 218 (2009).

[35]G. Lamour, A. Eftekhari-Bafrooei, E. Borguet, S. Souès, and A. Hamraoui, "Neuronal adhesion and differentiation driven by nanoscale surface free-energy gradients," Biomaterials **31**(14), 3762–3771 (2010).

[36]T. Bienville, J. F. Robillard, L. Belliard, I. Roch-Jeune, A. Devos, and B. Perrin, "Individual and collective vibrational modes of nanostructures studied by picosecond ultrasonics," Ultrasonics **44**, e1289–e1294 (2006).

[37]C. Jean, L. Belliard, L. Becerra, and B. Perrin, "Backward propagating acoustic waves in single gold nanobeams," Appl. Phys. Lett. **107**, 193103 (2015).

[38]X. J. Liang, A. Q. Liu, C. S. Lim, T. C. Ayi, and P. H. Yap, "Determining refractive index of single living cell using an integrated microchip," Sens. Actuators, A **133**, 349–354 (2007).

[39]G. Rohman, S. Ramtani, S. Changotade, C. Langueh, D. Lutomski, Y. Roussigne, F. Tetard, F. Caupin, and P. Djemia, "Characterization of elastomeric scaffolds developed for tissue engineering applications by compression and nanoindentation tests, $\mu$-Raman and $\mu$-Brillouin spectroscopies," Biomed. Opt. Express **10**(4), 1649–1659 (2019).

[40]K. Hayashi, C. G. Pack, M. K. Sato, K. Mouri, K. Kaizu, K. Takahashi, and Y. Okada, "Viscosity and drag force involved in organelle transport: Investigation of the fluctuation dissipation theorem," Eur. Phys. J. E **36**, 136 (2013).